



Plio-Pleistocene environmental variability in Africa and its implications for mammalian evolution

Andrew S. Cohen^{a,1}, Andrew Du^b, John Rowan^c, Chad L. Yost^d, Anne L. Billingsley^a, Christopher J. Campisano^e, Erik T. Brown^{f,g}, Alan L. Deino^h, Craig S. Feibelⁱ, Katharine Grant^j, John D. Kingston^k, Rachel L. Lupien^l, Veronica Muiruri^m, R. Bernhart Owenⁿ, Kaye E. Reed^e, James Russell^p, and Mona Stockhecke^f

Edited by David Jablonski, The University of Chicago, Chicago, IL; received April 22, 2021; accepted February 16, 2022

Understanding the climatic drivers of environmental variability (EV) during the Plio-Pleistocene and EV's influence on mammalian macroevolution are two outstanding foci of research in African paleoclimatology and evolutionary biology. The potential effects of EV are especially relevant for testing the variability selection hypothesis, which predicts a positive relationship between EV and speciation and extinction rates in fossil mammals. Addressing these questions is stymied, however, by 1) a lack of multiple comparable EV records of sufficient temporal resolution and duration, and 2) the incompleteness of the mammalian fossil record. Here, we first compile a composite history of Pan-African EV spanning the Plio-Pleistocene, which allows us to explore which climatic variables influenced EV. We find that EV exhibits 1) a long-term trend of increasing variability since ~3.7 Ma, coincident with rising variability in global ice volume and sea surface temperatures around Africa, and 2) a 400-ky frequency correlated with seasonal insolation variability. We then estimate speciation and extinction rates for fossil mammals from eastern Africa using a method that accounts for sampling variation. We find no statistically significant relationship between EV and estimated speciation or extinction rates across multiple spatial scales. These findings are inconsistent with the variability selection hypothesis as applied to macroevolutionary processes.

mammalian evolution | paleoclimate | variability selection | Africa | Plio-Pleistocene

Understanding the drivers of African environmental variability (EV) over geological time scales in the Afrotropics and inferring how this variability may have influenced the evolution of African mammals, including hominins, are long-standing problems within paleoclimatology, paleobiology, and paleoanthropology (1–4). The relative roles of high-latitude (e.g., onset of northern hemisphere cooling, glaciation, and high-latitude thermohaline circulation) vs. low-latitude (e.g., insolation and changes in the Walker Circulation) forcing in driving the region's climate variability on multiple times scales have been the subject of vigorous debate (5–11). However, comprehensive, stacked records of African variability over the entirety of the Plio-Pleistocene transformation of global climate have not been available.

Hypotheses invoking EV as drivers of evolution have also been widely discussed in recent years (12–14). The variability selection hypothesis was originally devised to explain the morphological and behavioral adaptations of species in the context of environmental instability (13) but was subsequently expanded to include macroevolutionary processes over the same Plio-Pleistocene time scales of concern in paleoclimate debates. Potts and Faith (14) suggested that periods of high EV would have been a key force in driving the fragmentation and isolation of populations, which would ultimately lead to elevated rates of speciation and extinction. However, previous studies linking records of EV with the African hominin and mammalian fossil records have faced two major limitations: 1) spatially restricted and temporally imprecise paleoenvironmental data, and/or 2) estimations of turnover patterns without accounting for the incompleteness of the fossil record (i.e., assuming that first and last appearance dates represent true speciation and extinction dates, which becomes especially problematic with poor sampling) (15, 16).

In order to address the limitations imposed by spatial and temporal restrictions of individual paleoenvironmental records, we have developed a composite history of Pan-African EV spanning the last 5.3 million years (My). Our composite record is based on 31 well-resolved and long-duration (>450 ky) records of terrestrial environments from 17 locations around Africa (Fig. 1 and *SI Appendix*, Fig. S1). Additionally, we separately analyzed variability of tropical Pan-African sea surface temperatures (SSTs), a global benthic foraminiferal oxygen isotope compilation ($\delta^{18}\text{O}_b$), insolation (March 21 daily means for 0°N, 15°N, 30°N, and 65°N used to represent combined effects of orbital parameters on insolation), and records of atmospheric CO₂, as these variables

Significance

We have developed an Africa-wide synthesis of paleoenvironmental variability over the Plio-Pleistocene. We show that there is strong evidence for orbital forcing of variability during this time that is superimposed on a longer trend of increasing environmental variability, supporting a combination of both low- and high-latitude drivers of variability. We combine these results with robust estimates of mammalian speciation and extinction rates and find that variability is not significantly correlated with these rates. These findings do not currently support a link between environmental variability and turnover and thus fail to corroborate predictions derived from the variability selection hypothesis.

Author contributions: A.S.C., A.D., and J. Rowan designed research; A.S.C., A.D., J. Rowan, C.L.Y., A.L.B., C.J.C., E.T.B., A.L.D., C.S.F., K.G., J.D.K., R.L.L., V.M., R.B.O., J. Russell, and M.S. performed research; A.S.C., A.D., J. Rowan, and C.L.Y. analyzed data; and A.S.C., A.D., J. Rowan, C.L.Y., A.L.B., C.J.C., E.T.B., A.L.D., C.S.F., K.G., J.D.K., R.L.L., R.B.O., K.E.R., and J. Russell wrote the paper.

The authors declare no competing interest.

This article is a PNAS Direct Submission.

Copyright © 2022 the Author(s). Published by PNAS. This article is distributed under [Creative Commons Attribution-NonCommercial-NoDerivatives License 4.0 \(CC BY-NC-ND\)](https://creativecommons.org/licenses/by-nc-nd/4.0/).

¹To whom correspondence may be addressed. Email: cohen@email.arizona.edu.

This article contains supporting information online at <http://www.pnas.org/lookup/suppl/doi:10.1073/pnas.2107393119/-/DCSupplemental>.

Published April 11, 2022.

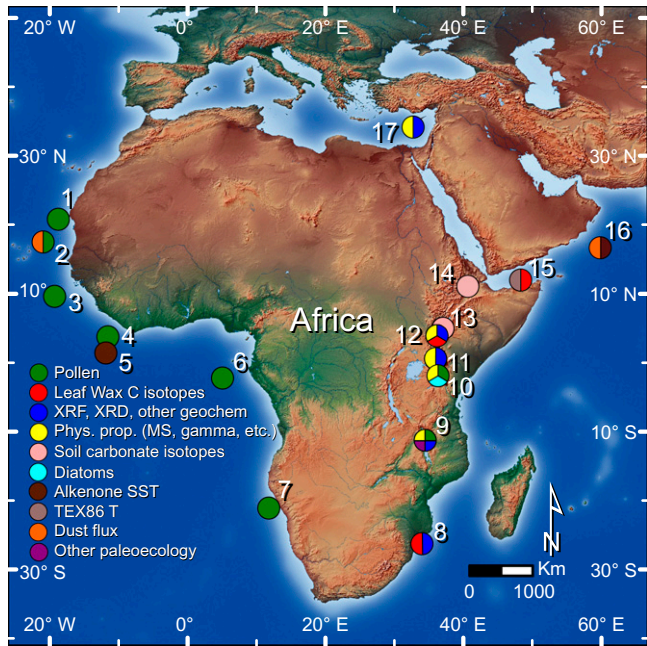


Fig. 1. Paleoenvironmental data sources and types. Circles indicate locations where records (core or outcrop) were collected. Color codes indicate the type of record. Data sources and further information on specific sites and records are given in [Dataset S1](#) and [SI Appendix, Fig. S1](#). Site key: 1) ODP658; 2) ODP659; 3) GIK16415-2; 4) GIK16776-1; 5) ODP662; 6) GIK16867; 7) ODP1082; 8) MD-96-2048; 9) MAL-1B/1C; 10) MAG-2A; 11) BTB-1A; 12) WTK-1A; 13) Omo R./Lake Turkana Region (Ethiopia/Kenya); 14) Afar Region (Ethiopia); 15) DSDP231; 16) ODP721/722; 17) ODP967.

are widely discussed records reflecting climatic variability on a global scale, which in turn can potentially influence African EV (3, 17–19) ([Dataset S1](#)). We recognize that the African records reflect a combination of climate, tectonism, volcanism, or other processes, all of which in principle can impact the variability of environmental conditions experienced by mammals (20). To calculate EV for each dataset, we first standardized the data to z-scores and then calculated interquartile ranges (IQRs) for the data within each time bin at three durations: 20, 100, and 250 ky ([SI Appendix, Fig. S2](#) and [Dataset S2](#); results do not change if we use the mean absolute deviation instead of z-scores: [SI Appendix, Fig. S3](#)). To develop a stacked, composite record of EV, we averaged IQRs for each bin across all records. We focused on records reflecting terrestrial environmental conditions collected from eastern Africa, the western Indian Ocean, and the eastern Mediterranean (hereafter EAIM), whose provenance is directly comparable to the mammalian records analyzed here. However, we also provide a composite of western African environmental variability, given the potential differences between these regions (10).

Regarding the second limitation of the incompleteness of the fossil record, we compiled a site-based occurrence dataset for eastern African mammalian herbivore species (orders Artiodactyla, Perissodactyla, and Proboscidea) spanning the last 3.75 My ($n = 84$ sites, [Dataset S3](#) and [SI Appendix, Fig. S4](#)). Herbivore taxa were used because they are the richest components of eastern African fossil assemblages (our dataset has >350 taxa), are primary consumers, meaning that they should be the most sensitive to climate/environmental change, and have figured widely in discussions of African faunal turnover patterns (1, 15, 16, 21, 22). Mammal data were aggregated into 250-ky bin durations for analysis, which is the best resolution possible for the current comprehensive mammal fossil record and similar to the bin durations

used in a recent study of eastern African mammalian turnover (22). We analyzed these mammal data using a capture–mark–recapture model (23–25) to estimate time-varying speciation and extinction probabilities, while simultaneously estimating, and thus accounting for, time-varying sampling probabilities (all estimated probabilities are equivalent to rates for our purposes).

Because the variability selection hypothesis has previously been tested with EV records at various spatial scales (i.e., global to regional) (14), we assessed the relationship between each of five EV variables (global: insolation, $\delta^{18}\text{O}_b$, Paleo CO_2 ; regional: stacked IQR–Pan-tropical African SSTs, stacked IQR–EAIM) with each of the estimated speciation and extinction probabilities. The EV variables were first rebinned at 250-ky resolution to match the mammalian data and then compared to the estimated probabilities using cross-correlations, where each probability lags each EV variable by up to two time bins (0.5 My maximum). Some recent arguments favoring the variability selection hypothesis suggest it may operate at the basinal (as opposed to regional/global) scale, linking local EV (which may encompass factors such as local topographic and hydrologic change, in addition to climate) to species turnover (13, 20). To test variability selection at the individual basin scale, we repeated our capture–mark–recapture and cross-correlation analyses for the mammalian and $\delta^{13}\text{C}$ paleosol carbonate EV records from the Turkana Basin from 4.25 to 1 Ma (250-ky bin size). This is the only basin-scale record with a long enough duration and high enough temporal resolution for our analyses.

Results

Climatic Correlates of African Environmental Variability. Our analysis of stacked IQR variability at the 100-ky bin resolution illustrates several features of Pan-African EV since the Pliocene (Fig. 2A). Most importantly, we note a long-term, statistically significant trend of increasing EV since ~3.7 Ma (linear model of EV against time: $R^2 = 0.293$, $P < 0.001$). Prior to this, the number of records integrated into each time bin of our dataset is quite small ($n = 2$ to 5), hence we refrain from interpreting the older portion of the record. The trend of increasing variability since the late Pliocene is also evident in the EAIM records (Fig. 2B). It is also observed in the subset of records that were not astronomically tuned directly to the utilized record (Fig. 2C). Western African variability, in contrast, generally increases between ~3.0 and 0.6 Ma and then declines sharply (Fig. 2D). The EAIM data show statistically robust relationships at the 100-ky bin duration with marine $\delta^{18}\text{O}_b$ (Fig. 2E and [SI Appendix, Table S1](#)), regional SSTs (Fig. 2F), and equatorial mean daily (March 21) insolation (Fig. 2G). IQR variability of insolation is almost identical between the equator, 15°N, 30°N, and 65°N, thus the choice of latitude does not affect these results in any appreciable way ([SI Appendix, Figs. S5](#) and [S6](#)). CO_2 variability ([Dataset S2](#)) is not correlated with any of the African terrestrial EV records at any bin size, although the short duration of the ice-core CO_2 record limits this analysis.

To assess the relationship between insolation and the EV records, we analyzed the highest possible resolution bin size (20 ky) that can, in principle, detect 100- and 400-ky eccentricity cycles (although not the 21-ky precession cycle nor the 41-ky obliquity cycle). The 20-ky bin data ([SI Appendix, Fig. S7](#)), which meet our data density and record duration criteria for the 3.22 to 0 Ma interval (see [Materials and Methods](#)), are illustrated with Morlet wavelet time series analyses (Fig. 3). Strong 400-ky cyclicity is apparent in the Pan-African (Fig. 3A and B), and

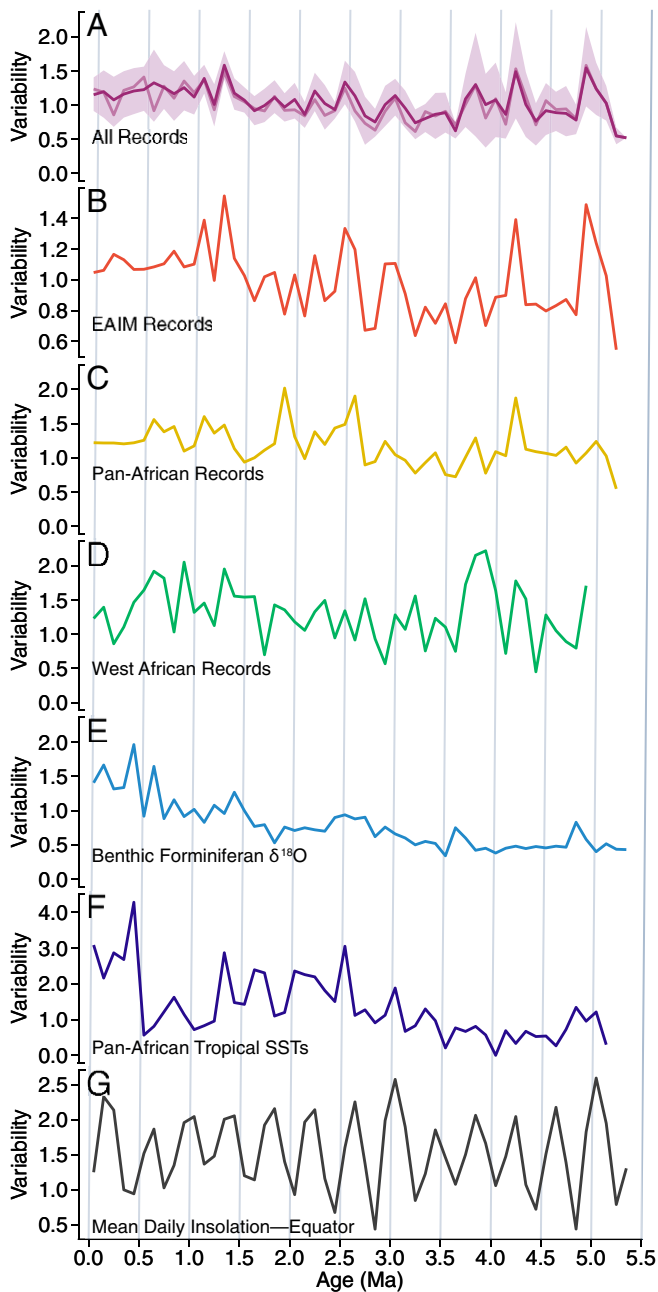


Fig. 2. Interquartile ranges of z-scores (“variability”) for all records using 100-ky bins. (A) Mean (dark purple) variabilities for all terrestrially derived sites (no SSTs; median in light purple) plus upper and lower 95% confidence intervals (1,000 bootstraps). (B) Mean variabilities for eastern Africa + Indian Ocean + eastern Mediterranean (EAIM) records (no SSTs). (C) Same as B but for all Pan-African records whose records were not directly astronomically tuned and also excluding SSTs. (D) Same as B but for Western African records. (E) Variabilities of z-scores for the benthic foraminiferan $\delta^{18}\text{O}_b$ records. (F) Same as B but for Pan-African tropical sea surface temperatures. (G) Same as E but for mean daily insolation at equator.

EAIM records (Fig. 3C), consistent with prior inferences based on more limited data (14). The 400-ky cycle in the records aligns with that of insolation (Fig. 3D). There is also a strong correlation between the IQR variability means of individual 20-ky bins in the combined EAIM records and insolation (*SI Appendix*, Fig. S8). Importantly, this 400-ky periodicity is evident in the Pan-African records whose underlying age models are not reliant on astronomical tuning (Fig. 3B). There are also intervals in the African terrestrial variability records that show significant cyclicality

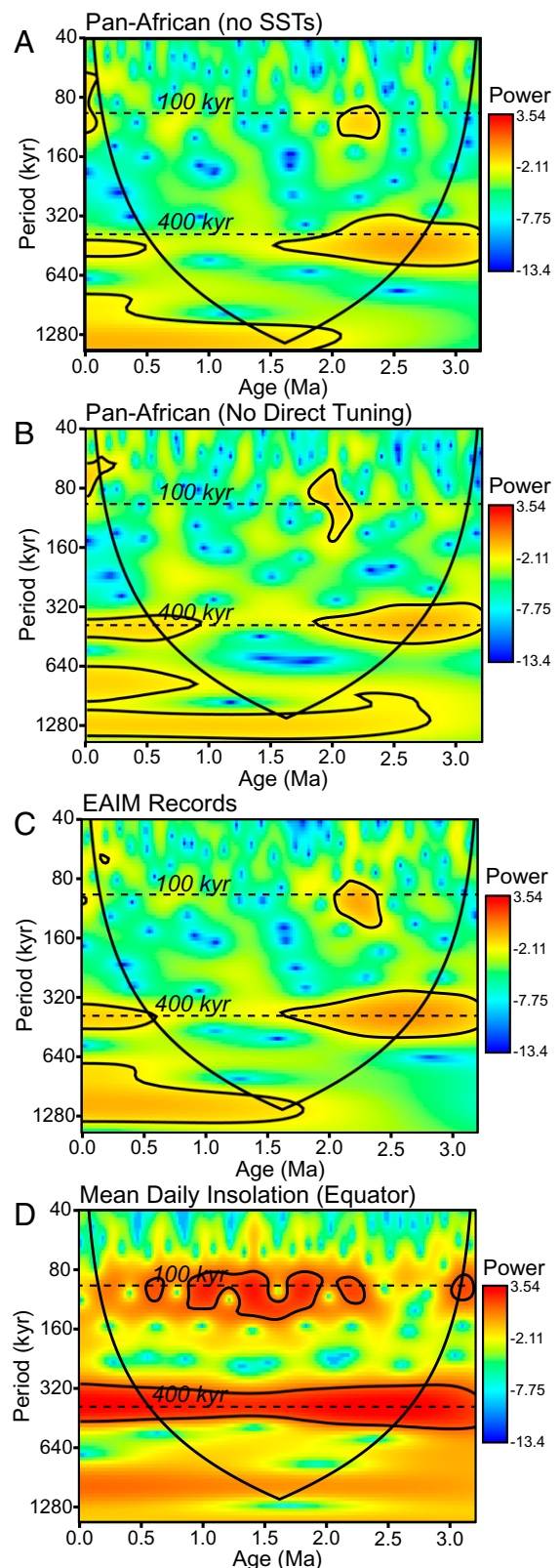


Fig. 3. (A) Wavelet analysis (equal and continuous bin spacing, Morlet wavelet) of 20-ky bin stacked IQR (variability) time series for all Pan-African records shown in Fig. 1 and *Dataset S1* except SSTs for the period 3.21 to 0 Ma (the interval for which the number of available EAIM 20-ky bin records is consistently >6). (B) Same as A but removing records for which the dataset itself was directly astronomically tuned. (C) Same as A but only EAIM data. (D) Wavelet analysis for 20-ky bin variability in mean daily insolation at 0°N , calculated in 1-ky time steps for comparison with other panels. Cones of influence and $P = 0.05$ significance level indicated by black lines.

in the 100-ky frequency band, although this is less consistent than the 400-ky band and shows a weaker relationship with insolation. Furthermore, the 100-ky frequency is not statistically significant when the tuned datasets are excluded from the analysis.

Our analyses thus show that Plio-Pleistocene Pan-African EV is correlated with long-term changes in global ice volume, tropical temperature, and seasonal insolation forcing. To further analyze these relationships, we performed a change-point analysis of both means and slopes (trends) of the stacked IQR EV datasets using 250-ky bins. The analysis identifies change points at 1.25 Ma for higher EV (means) and 2.5 Ma for increasing EV (slope) for the terrestrial Pan-African composite dataset (*SI Appendix, Fig. S9 A and B*). The terrestrial EAIM records (*SI Appendix, Fig. S9C*) identify change points at 1.5 Ma for higher EV (means) and 3.25 Ma for increasing EV (slope), the latter corresponding to the start of an overall increase in variability also noted earlier from higher-resolution binning (Fig. 2). A ~ 3.1 Ma change point has been previously observed in high-resolution vegetation and fire records from the Baringo Basin in eastern Africa (26, 27) and in regional dust records at about this same time (5). The transitions to greater variability in the African records starting at ~ 3.6 Ma is largely coincident with global changes toward greater ice volume and sea-surface temperature variability associated with the onset of northern high-latitude glaciation (28–31), although these high-latitude changes are variable in space and time and may in part be unrelated to ice buildup (32). The set of change points in the terrestrial African records between 3.25 and 2.5 Ma could suggest a similarly gradual transition in which different components of African climate and paleoenvironments shift in concert with high-latitude changes. Overall, our results are consistent with climate-modeling experiments (9, 33) that predict control of African precipitation through both seasonal insolation forcing and high-latitude climate variation.

Comparing Environmental Variability and Mammalian Evolution.

Estimated speciation and extinction probabilities for eastern African mammals show no clear trend through the Plio-Pleistocene (Fig. 4B). Both probabilities remain generally low, except for a spike in extinction probability in the 0.75 to 0.5 Ma bin. The mean speciation probability for all time bins is 0.15, whereas the mean extinction probability without the spike is 0.13 (using the lumped “cf.” taxonomic treatment; see *Materials and Methods*). Based on visual assessment, there is no relationship between the long-term increasing variability trend and turnover probabilities at the 250-ky resolution. This is quantitatively corroborated by cross-correlation analyses, comparing each of the speciation and extinction probabilities with each of the EV variables (EAIM, insolation, CO_2 , $\delta^{18}\text{O}_b$, Pan-tropical African SST). The mean of all 30 computed cross-correlation coefficients is -0.09 (standard deviation [SD] = 0.20), and no coefficients are statistically significant.

As with the regional analyses, Turkana Basin speciation and extinction probabilities for mammals show no trend through time and generally remain low, save for a speciation and extinction spike in the 3.75 to 3.5 Ma and 1.5 to 1.25 Ma time bins, respectively (speciation and extinction means without their respective spikes are both 0.1 for the lumped “cf.” treatment) (Fig. 4D). The six cross-correlation estimates between each of these probabilities and Turkana paleosol $\delta^{13}\text{C}$ variability are low (mean = -0.02 ; SD = 0.33) and not statistically significant (*SI Appendix, Fig. S10 and Dataset S4*).

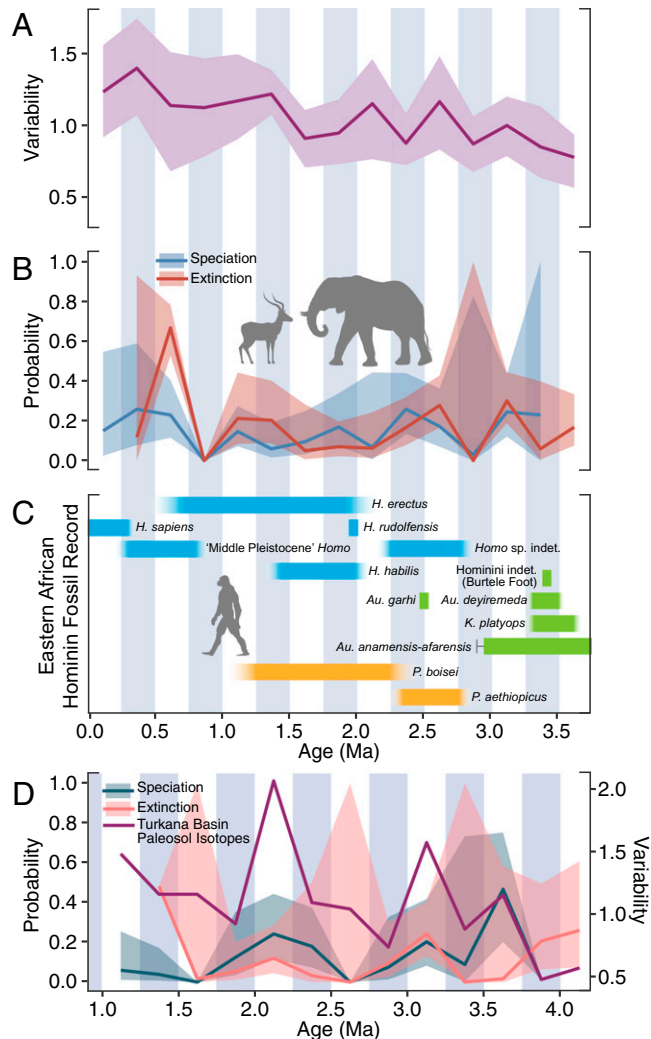


Fig. 4. Comparison of environmental variability records with time-dependent large mammalian turnover probabilities, estimated using a capture-mark-recapture model (Pradel's seniority model; see *Materials and Methods*). All plots use 250-ky time bins (alternating white and lilac vertical bars) and include estimates with their 95% confidence intervals (except variability from the Turkana Basin $\delta^{13}\text{C}$ paleosol carbonate record). (A) EAIM stacked IQRs of z-scores (environmental variability). (B) Speciation and extinction probabilities for eastern African mammals. (C) Eastern African hominin fossil record. *Au.*, *Australopithecus*; *H.*, *Homo*; *K.*, *Kenyanthropus*; *P.*, *Paranthropus*. For the *Au. anamensis-afarensis* lineage range, the hard edge represents the last appearance date, and whisker denotes the 95% confidence interval (51). Confidence intervals on speciation and extinction dates have not been estimated for other hominin taxa. (D) Speciation and extinction probabilities for Turkana Basin mammals only, compared with environmental variability from Turkana Basin paleosol isotopes. All estimated speciation/extinction probabilities use the lumped “cf.” taxonomic treatment. See text for further discussion.

Discussion

When exploring the spatial scales that variability selection has been argued to operate at—global and regional EV influencing regional faunas and basin-scale EV influencing basin-scale faunas—we currently find no statistical support for an association between available EV records and long-term mammalian turnover in eastern Africa, the region of the continent with the richest and most continuous Plio-Pleistocene fossil record (*SI Appendix, Fig. S10 and Dataset S3*). These findings are inconsistent with predictions derived from the variability selection hypothesis as they relate to macroevolution (2, 14), wherein one would expect a significant, positive relationship between EV and rates of speciation and extinction through time.

Our findings, however, do not eliminate the possibility that higher-frequency variability (e.g., eccentricity- or precession-scale), which is clearly evident in our composite record in the 20-ky bin analysis, drove faunal turnover events during the Plio-Pleistocene. Indeed, empirical data compilations (14) suggest that some aspects of variability selection could play out on these shorter timescales. Likewise, it remains an open question whether terrestrial biotas may have responded to heightened EV during the Plio-Pleistocene through microevolutionary (populational) shifts in traits or spatial distributions that are not reflected in speciation and extinction records (34). Rigorous testing of the relationship between subcentricity or shorter-term cycles as a driver of macroevolution must await a more resolved fossil record. Here, we have made maximal effort to ensure that we tailored the spatiotemporal scale of our question to that of the available data (35), and extrapolating our findings to shorter time scales of environmental and evolutionary change would be premature.

Our cross-correlation analyses ignored error and uncertainty in the time series of different EV records and speciation and extinction probabilities. Such an omission artificially inflates the magnitudes of cross-correlation coefficients and decreases P values (36). Despite these biases toward statistically significant results, none of our cross-correlations are significant (i.e., our results are in the opposite direction of the bias). Thus, our cross-correlation results are robust and would yield lower-magnitude coefficients and larger P values if we incorporated time series error into our analyses. We also note that the time series in our cross-correlations are fairly short: there are only 14 and 12 data points in the eastern African and Turkana analyses, respectively. While we are constrained by the size and temporal resolution of our dataset, we recognize that our short time series produce less precise parameter estimates and low statistical power (37), and the future addition of more data may yield statistically significant cross-correlation estimates. Lastly, we acknowledge that our cross-correlation analyses are correlative and do not directly address the question of whether environmental variability drove speciation and extinction rates. Inferring causality would require more sophisticated analyses (e.g., testing for Granger causality) (49), and this should be the goal of future studies.

We estimated rates of speciation and extinction for the mammalian fossil record using methods that can account for the incomplete nature of this record. The hominin record itself, however, is particularly incomplete, and most diversity patterns seem to be shaped by sampling biases (38), highlighting the problematic practice of ascribing particular environmental changes as forcing factors for changes observed in human evolutionary history (Fig. 4C). Nevertheless, with these caveats in mind and taking the eastern African hominin fossil record at face value, the overall pattern of hominin speciation and extinction does not show any obvious trended increase over the last 3.7 My, which would be expected if EV were a key driver. Progress in understanding the role of environment in hominin evolutionary history awaits both theoretical and analytical advances (35) and continued fossil discoveries. Until then, drawing causal links between transitions in environmental and human evolutionary histories remains an elusive enterprise.

Conclusions

We generated a composite history of Pan-African EV spanning the last 5.3 My to evaluate its candidate climatic drivers and its possible role in influencing mammalian macroevolutionary

history. Using IQRs of z-scores from 31 highly resolved paleo-environmental datasets at three bin durations (20, 100, and 250 ky), we first demonstrate that African (and specifically eastern African) EV through the Plio-Pleistocene has two major components: 1) a 400-ky frequency component, correlated with seasonal insolation variability, superimposed on 2) a longer-term trend of increasing variability since ~ 3.7 Ma, coincident with rising variability in global ice volume and sea surface temperatures around Africa. We identified several significant change points in the pattern of variability, some of which correspond to the Plio-Pleistocene transition elsewhere, again suggesting global drivers for the history of African EV. Through analyses of a fossil dataset for Plio-Pleistocene eastern African mammalian herbivores spanning the last 3.75 My, we document no clear trend in speciation and extinction probabilities. Furthermore, our analysis of the last 3.75 My using 250-ky time bins did not demonstrate any statistically significant relationship between Plio-Pleistocene EV and estimated speciation or extinction rates at both the regional (eastern Africa) and basinal (Turkana Basin) scale. These findings do not currently support hypotheses linking EV with macroevolutionary aspects of faunal turnover in the African fossil record.

Materials and Methods

Environmental Variability Metrics. Analyzed datasets include those that were collected on the African continent (e.g., lacustrine diatom records), as well as records from marine cores from the margins of the continent that are derived from African sources (e.g., marine pollen records). A screening procedure (discussed along with other EV method details in the *SI*) was used to ensure sufficient data density in utilized records for the individual time bins within which variability was calculated. Time bins were arrayed starting at the present for a given bin size, and data falling on the older time bin boundary were included in a given bin (e.g., for 20 ky bins, 0 > to 20 ka, 20 > to 40 ka, etc.).

Multivariate ordination (correspondence analysis, CA), time series, correlation, and autocorrelation analyses of environmental variability data were all implemented in Paleontological Statistics (PAST) 4.03 (39). CA was used to reduce raw pollen datasets to a first CA axis of inertia for variability analysis, combining all terrestrial pollen types provided from the original published datasets but eliminating *Rhizophora* (marine/brackish mangroves) from the sums where present because of overrepresentation bias relative to fully terrestrial floras. REDFIT spectral analysis uses the REDFIT procedure (40) in which the time series incorporates a first-order autoregressive process. For the REDFIT spectral analysis, we used the rectangular window function, computed 1,000 Monte Carlo random realizations, and used a 95% χ^2 threshold to assess significance. The continuous wavelet transform used a Morlet function (shape of mother wavelet wavenumber 6) and calculated the cone of influence (boundary of possible edge effects) with a $P = 0.05$ significance level (white noise null hypothesis). Correlation analyses were calculated using Pearson's r in PAST.

Change Point Analysis. Change points in the mean and slope for the 250-ky bin variability datasets were individually calculated using the *findchangepts* function from the Signal Processing Toolbox in MATLAB ver. R2020b.

Mammalian Fossil Data. We compiled species-level occurrence data from a recently published dataset (41) for terrestrial mammalian herbivores (orders Artiodactyla, Perissodactyla, and Proboscidea) spanning the last 5 My in eastern Africa. While a species' occurrence at a site indicates its presence there, an absence could be due to a true absence or an undetected presence. This distinction is accounted for by our capture-mark-recapture model by explicitly modeling sampling probability through time (see "Turnover Analyses" below). We have not included mammalian records from other regions of Africa (e.g., South Africa) because they lack the long sequences and high chronological resolution available in eastern Africa. We specifically focused our turnover analyses on herbivores for four primary reasons. First, herbivores comprise the most abundant and species-rich mammal clades found at late Cenozoic fossil sites in eastern Africa. Second, the vast majority of fossil herbivore taxa were relatively large-bodied (often >50 kg), meaning

that they are less prone to suffer from the more impactful taphonomic, survey, and collection biases that shape the recovery of smaller-bodied and/or rarer taxa (42), including many carnivorans, primates, and micromammals. Third, as primary consumers, the ecological niches of herbivore taxa are closely tied to their local environments, meaning that they should be among the most sensitive mammalian taxa to climatic and/or environmental change in the past (43). Indeed, many studies aiming to establish correlations between climate change and mammalian turnover in the African record often focus on one or more herbivore clades, e.g., bovids (1, 21, 22, 44). Finally, the Plio-Pleistocene herbivore faunas of eastern Africa are highly provincial—very few species are shared with contemporaneous sites from South or Central Africa. For example, Rowan et al. (45) show that among bovids—the most abundant and speciose fossil mammals in Neogene African deposits—very few (<10 to 15%) species were shared between eastern and southern Africa when aggregating data into 500-ky time bins from 3 to 1 Ma. This means that for most taxa in our analyses, cases where immigration/emigration are confused with speciation/extinction are few.

Our dataset (Dataset S3 and SI Appendix, Fig. S4) represents an extensive compilation of eastern African mammalian records ($n = 103$ sites total, spanning >350 taxa). For each site, we collected absolute age estimates (mainly from upper and lower bounding $^{40}\text{Ar}/^{39}\text{Ar}$ dated tephra) and aggregated sites by mean age into 250-ky bins for analysis (mean ages falling on an older bin boundary were placed into that bin). While our composite climate records were available at higher resolutions (i.e., 20 and 100 ky), 250 ky is the shortest bin duration possible for turnover analysis. For the final regional-scale analyses, we used only sites dating to 3.75 to 0 Ma ($n = 84$ sites) because the climate and fossil records are poorly sampled in earlier time intervals at this scale. For the final basin-scale analysis of Turkana mammals, we analyzed sites dating 4.25 to 1 Ma ($n = 33$ sites).

Some of the species records in our dataset include open nomenclature (e.g., “cf.” and “aff.”) that have been variably treated in past studies. To test for the effect of open nomenclature on our results, we generated two versions of the dataset: the first version (used for the main text analyses) lumped “cf.” records with their likely taxon (e.g., *Kobus cf. sigmoidalis* → *Kobus sigmoidalis*) with the understanding that this modifier is most often used to denote probable records that simply lack diagnostic morphology (46); the second version dropped “cf.” records completely (>20% of the dataset). Both versions dropped indeterminate (“sp.” and “indet.”) records but retained “aff.” records, with the understanding that this modifier is used to denote a species related to, but distinct from, a known species. While it is possible that “aff.” records of a taxon (e.g., *Kobus aff. sigmoidalis*) could represent separate taxa (i.e., two or more taxa similar to *Kobus sigmoidalis* but distinct from one another), we consider this situation unlikely for two reasons: 1) many of the “aff.” records come from the same stratigraphic sequence and were designated as such by the same specialist; and 2) our database relies on up-to-date compilations by specialists working on fossil collections across several sites, so introduced noise from variation in taxonomic practice is minimized. Speciation and extinction probabilities calculated using the two versions of the dataset were highly correlated (eastern African mammals: Pearson’s $r = 0.91$ for speciation and 0.94 for extinction; Turkana mammals: Pearson’s $r = 0.99$ for speciation and 0.99 for extinction) indicating that our turnover analyses are robust to variation in taxonomic treatment (see SI Appendix, Fig. S11). Therefore, we use only the lumped “cf.” treatment in our cross-correlation analyses (see below).

Turnover Analyses. We used a capture–mark–recapture model (23) to jointly estimate time-dependent speciation, extinction, and sampling probabilities for our occurrence matrix of large fossil mammals from eastern Africa (3.75 to 0 Ma; 250-ky bins). Specifically, we used Pradel’s seniority model (24) to estimate: 1) extinction probability as one minus the probability a given taxon survives from time i to $i + 1$ (i.e., survival probability: φ_i); 2) speciation probability as one minus the probability a given taxon extant at time i was also extant at time $i - 1$ (i.e., seniority probability: γ_i); and 3) sampling probability (p_i) as the probability a given taxon will be sampled in time i , given that it was extant then. Extinction probability is interpreted as the probability that any given taxon will go extinct from time i to $i + 1$ (or the expected proportion of taxa that go extinct during this time period), and speciation probability is interpreted as the probability any given taxon will speciate from time $i - 1$ to i (or the expected proportion of taxa that speciated during this time period). We allowed all three probabilities to vary through time but not across taxa, resulting in 43 total

estimated parameters for 187 taxa over 15 time bins for the lumped “cf.” treatment, and 43 estimated parameters for 177 taxa over 15 time bins for the dropped “cf.” treatment. For the Turkana analyses (4.25 to 1 Ma; 250-ky bins), we estimated 37 total estimated parameters for 96 taxa over 13 time bins for the lumped “cf.” treatment, and 37 estimated parameters for 93 taxa over 13 time bins for the dropped “cf.” treatment. We estimated probabilities using the RMark (v 2.2.7) R package (25) with code adapted from Smiley (47).

Cross-Correlation Analyses. We used the R *ccf* function to conduct cross-correlation analyses, comparing each of the estimated speciation and extinction probabilities for eastern African mammals with each of the five EV variables (insolation, 65°N , 35°E ; $^{18}\text{O}_b$; Paleo CO_2 ; variability means IQR-SSTs; variability means IQR-EAIM) for a total of 10 comparisons using the lumped “cf.” treatment only. Our analyzed time series contained 14 data points each, and we looked at lags of up to two time bins (i.e., 0.5 My), where a lag indicates younger speciation/extinction probabilities are compared to older EV variables. For the basin-scale analyses, we compared each of the estimated speciation and extinction probabilities for Turkana mammals with paleosol $\delta^{13}\text{C}$ variability for a total of two comparisons using the lumped “cf.” treatment only. Each time series contained 12 data points, and we calculated cross-correlations up to two lags (i.e., 0.5 My).

It is well known that the type I error rate of estimated cross-correlation coefficients increases with the magnitude of autocorrelation in both of the compared time series (48, 49). Therefore, we used an adjusted significance threshold, defined as $\pm 1.96 \sqrt{(1 + 2 \sum_{k=1}^m \rho_k(x)\rho_k(y)) / n}$, where k indicates the lag number, n is the length of the time series, $\rho_k(x)$ and $\rho_k(y)$ are the estimated autocorrelation coefficients for the two time series at lag k (autocorrelation coefficients estimated using the *acf* R function), and $m = \lfloor 10 \log_{10} n \rfloor$ (i.e., the default maximum lag number in the *acf* function) (48, 49). If there is no autocorrelation at all lags for at least one of the time series (i.e., either $\rho_k(x)$ or $\rho_k(y)$ equals zero for all k), the equation reduces to the conventional cross-correlation significance limit of $\pm 1.96 / \sqrt{n}$. Because this method assumes that both time series are stationary, we first detrended each series by taking the residuals from a LOWESS regression modeling the time series variable as a function of time (using the *lowess* R function and a smoothing span of 2/3) (SI Appendix, Figs. S12 and S13).

The mammalian turnover and cross-correlation analyses were done in R v4.1.0 (50).

Data Availability. All data are available in the form of figures in the main text or supporting information. Original sources for published data from which the variability analyses were derived are provided in Dataset S1 and in the individual headers of Dataset S2. Raw Multisensor Core Logging data for the Magadi (MAG), Baringo/Tugen Hills/Barsemoi (BTB), and West Turkana (WTK) core analyses are available at Open Science Framework sites <https://dx.doi.org/10.17605/OSF.IO/D384T>, <https://dx.doi.org/10.17605/OSF.IO/ANFYW>, and <https://dx.doi.org/10.17605/OSF.IO/B8QF2>, respectively. Climate variability data for the cross-correlation analyses and faunal data are provided in GitHub at <https://github.com/andrewdu1/VariabilitySelection>, as well as R scripts for cleaning the faunal data and transforming them into species-by-time matrices, running the capture–mark–recapture analyses, and running the cross-correlation analyses.

ACKNOWLEDGMENTS. We thank Laura Soul for discussions about capture–mark–recapture methods and William Dunsmuir, Eric Friedlander, and Kung-Sik Chan for answering a question about the variance of cross-correlation estimates. This is publication 51 of the Hominin Sites and Paleolakes Drilling Project (HSPDP). This research was supported by NSF Division of Earth Sciences Grant EAR 1338553 and the Hong Kong Research Grants Council (Grant HKBU12300815). K.G. is supported by the Australian Research Council (Grant DE190100042).

Author affiliations: ^aDepartment of Geosciences, University of Arizona, Tucson, AZ 85721; ^bDepartment of Anthropology & Geography, Colorado State University, Fort Collins, CO 80523; ^cDepartment of Anthropology, University at Albany, Albany, NY 12222; ^dDepartment of Earth & Environmental Systems, Indiana State University, Terre Haute, IN 47809; ^eSchool of Human Evolution & Social Change, Institute of Human Origins, Arizona State University, Tempe, AZ 85287; ^fLarge Lakes Observatory, University of Minnesota Duluth, Duluth, MN 55812; ^gDepartment of Earth and Environmental Sciences, University of Minnesota Duluth, MN 55812; ^h $^{40}\text{Ar}/^{39}\text{Ar}$ Laboratory, Berkeley Geochronology Center, Berkeley, CA 94709; ⁱDepartment of Earth and Planetary Sciences, Rutgers University, Piscataway, NJ 08854; ^jResearch School of Earth Sciences, Australian National University, Canberra, ACT 2601, Australia; ^kDepartment of Anthropology, University of Michigan, Ann Arbor, MI 48109; ^lDivision of Biology and Paleo Environment, Lamont Doherty Earth Observatory, Columbia University, Palisades, NY 10964; ^mEarth Sciences Department, National Museums of Kenya, Nairobi, 00100, Kenya; ⁿDepartment of Geography, Hong Kong Baptist University, Hong Kong; and ^oDepartment of Earth Environmental and Planetary Sciences, Brown University, Providence, RI 02912

1. E. S. Vrba, The fossil record of African antelopes (Mammalia, Bovidae) in relation to human evolution and paleoclimate in *Paleoclimate and Evolution with Emphasis on Human Origins*, E. S. Vrba, G. H. Denton, T. C. Partridge, L. H. Burckle, Eds. (Yale University Press, 1995), pp. 285–424.
2. R. Potts, Variability selection in hominid evolution. *Evol. Anthropol.* **7**, 81–96 (1998).
3. P. deMenocal, African climate change and faunal evolution during the Plio-Pleistocene. *Earth Planet. Sci. Lett.* **220**, 3–24 (2004).
4. J. D. Kingston, Shifting adaptive landscapes: Progress and challenges in reconstructing early hominid environments. *Am. J. Phys. Anthropol.* **134** (suppl. 45), 20–58 (2007).
5. M. H. Trauth, J. C. Larrasoana, M. Mudelsee, Trends, rhythms and events in Plio-Pleistocene African climate. *Quat. Sci. Rev.* **28**, 399–411 (2009).
6. L. D. Pena, S. L. Goldstein, Thermohaline circulation crisis and impacts during the mid-Pleistocene transition. *Science* **345**, 318–322 (2014).
7. D. J. Nash *et al.*, African hydroclimatic variability during the last 2000 years. *Quat. Sci. Rev.* **154**, 1–22 (2016).
8. S. E. Nicholson, Climate and climatic variability of rainfall over eastern Africa. *Rev. Geophys.* **55**, 590–635 (2017).
9. J. E. Kutzbach *et al.*, African climate response to insolation and glaciation: 140,000-year climate simulation with implications for early human environments. *Proc. Natl. Acad. Sci. U.S.A.* **117**, 2255–2264 (2020).
10. S. Kaboth-Bahr *et al.*, Paleo-ENSO influence on African environments and early modern humans. *Proc. Natl. Acad. Sci. U.S.A.* **118**, e2018277118. (2021).
11. H. J. L. van der Lubbe *et al.*, Indo-Pacific Walker circulation drove Pleistocene African aridification. *Nature* **598**, 618–623 (2021).
12. M. Grove, Speciation, diversity, and Mode 1 technologies: The impact of variability selection. *J. Hum. Evol.* **61**, 306–319 (2011).
13. R. Potts, Hominin evolution in settings of strong environmental variability. *Quat. Sci. Rev.* **73**, 1–13 (2013).
14. R. Potts, J. T. Faith, Alternating high and low climate variability: The context of natural selection and speciation in Plio-Pleistocene hominin evolution. *J. Hum. Evol.* **87**, 5–20 (2015).
15. M. Fortelius *et al.*, An ecometric analysis of the fossil mammal record of the Turkana Basin. *Philos. Trans. R. Soc. Lond. B Biol. Sci.* **371**, 20150232 (2016).
16. A. K. Behrensmeyer, N. E. Todd, R. Potts, G. E. McBrinn, Late Pliocene faunal turnover in the Turkana Basin, Kenya and Ethiopia. *Science* **278**, 1589–1594 (1997).
17. M. H. Trauth *et al.*, High- and low-latitude forcing of Plio-Pleistocene East African climate and human evolution. *J. Hum. Evol.* **53**, 475–486 (2007).
18. M. W. Blome, A. S. Cohen, C. A. Tryon, A. S. Brooks, J. Russell, The environmental context for the origins of modern human diversity: A synthesis of regional variability in African climate 150,000–30,000 years ago. *J. Hum. Evol.* **62**, 563–592 (2012).
19. H. M. Liddy, S. J. Feakins, J. E. Tierney, Cooling and drying in northeast Africa across the Pliocene. *Earth Planet. Sci. Lett.* **449**, 430–438 (2016).
20. R. Potts *et al.*, Increased ecological resource variability during a critical transition in hominin evolution. *Sci. Adv.* **6**, eabc8975 (2020).
21. R. Bobe, G. G. Eck, Responses of African bovids to Pliocene climatic change. *Paleobiology* **27**, 1–47 (2001).
22. F. Bibi, W. Kiessling, Continuous evolutionary change in Plio-Pleistocene mammals of eastern Africa. *Proc. Natl. Acad. Sci. U.S.A.* **112**, 10623–10628 (2015).
23. L. H. Liow, J. D. Nichols, "Estimating rates and probabilities of origination and extinction using taxonomic occurrence data: Capture-mark-recapture (CMR) approaches" in *Quantitative Methods in Paleobiology, Paleo. Soc. Short Course*, J. Alroy, G. Hunt, Eds. (Paleontological Society 16, 2010), pp. 81–94.
24. R. Pradel, Utilization of capture-mark-recapture for the study of recruitment and population growth rate. *Biometrics* **52**, 703–709 (1996).
25. J. L. Laake, "RMark: An R interface for analysis of capture-recapture data with MARK" (AFSC Processed Report 2013-01 Alaska Fish. Sci. Cent., NOAA, Natl. Mar. Fish. Serv., Seattle, 2013).
26. R. Lupien *et al.*, Vegetation change in the Baringo Basin, East Africa across the onset of Northern Hemisphere glaciation 3.3–2.6 Ma. *Palaeogeog. Palaeoclim. Palaeoecol.* **570**, 109426 (2021).
27. C. L. Yost *et al.*, Phytoliths, pollen, and microcharcoal from the Baringo Basin, Kenya reveal savanna dynamics during the Plio-Pleistocene transition. *Palaeogeog. Palaeoclim. Palaeoecol.* **570**, 109779 (2021).
28. M. A. Maslin, X. S. Li, M.-F. Loutre, A. Berger, The contribution of orbital forcing to the progressive intensification of northern hemisphere glaciation. *Quat. Sci. Rev.* **17**, 411–426 (1998).
29. M. Mudelsee, M. Raymo, Slow dynamics of the Northern Hemisphere glaciation. *Paleoceanography* **20**, PA4022 (2005).
30. S. De Schepper, P. L. Gibbard, U. Salzmann, J. Ehlers, A global synthesis of the marine and terrestrial evidence for glaciation during the Pliocene Epoch. *Earth Sci. Rev.* **135**, 83–102 (2014).
31. E. Ruggieri, T. Herbert, K. T. Lawrence, C. E. Lawrence, Change point method for detecting regime shifts in paleoclimatic time series: Application to $\delta^{18}\text{O}$ time series of the Plio-Pleistocene. *Paleocean. Paleoclim.* **24**, PA1204 (2009).
32. M. Trauth *et al.*, Northern Hemisphere glaciation, African climate and human evolution. *Quat. Sci. Rev.* **268**, 107095 (2021).
33. B. L. Otto-Bliesner *et al.*, Coherent changes of southeastern equatorial and northern African rainfall during the last deglaciation. *Science* **346**, 1223–1227 (2014).
34. M. Grove, Palaeoclimates, plasticity, and the early dispersal of *Homo sapiens*. *Quat. Int.* **369**, 17–37 (2015).
35. J. T. Faith *et al.*, Rethinking the ecological drivers of hominin evolution. *Trends Ecol. Evol.* **36**, 797–807 (2021).
36. B. K. Butland *et al.*, Measurement error in time-series analysis: A simulation study comparing modelled and monitored data. *BMC Med. Res. Methodol.* **13**, 136 (2013).
37. P. Legendre, "Developments in environmental modelling" in *Numerical Ecology* (Elsevier, ed. 3, 2012).
38. S. J. Maxwell, P. J. Hopley, P. Upchurch, C. Soligo, Sporadic sampling, not climatic forcing, drives observed early hominin diversity. *Proc. Natl. Acad. Sci. U.S.A.* **115**, 4891–4896 (2018).
39. Ø. Hammer, *PAST Paleontological Statistics*. <https://past.en.fo4d.com/windows>. Accessed 28 February 2021.
40. M. Schulz, M. Mudelsee, REDFIT: Estimating red-noise spectra directly from unevenly spaced paleoclimatic time series. *Comput. Geosci.* **28**, 421–426 (2002).
41. J. T. Faith, J. Rowan, A. Du, P. L. Koch, Plio-Pleistocene decline of African megaherbivores: No evidence for ancient hominin impacts. *Science* **362**, 938–941 (2018).
42. A. K. Behrensmeyer, S. M. Kidwell, R. A. Gastaldo, Taphonomy and paleobiology. *Paleobiology* **26**, 103–147 (2000).
43. M. J. Greenacre, E. S. Vrba, Graphical display and interpretation of antelope census data in African wildlife areas, using correspondence analysis. *Ecology* **65**, 984–997 (1984).
44. R. Bobe, A. K. Behrensmeyer, G. G. Eck, J. M. Harris, "Patterns of abundance and diversity in late Cenozoic bovids from the Turkana and Hadar Basins, Kenya and Ethiopia" in *Hominin Environments in the East African Pliocene: An Assessment of the Faunal Evidence*, R. Bobe, Z. Alemseged, A. K. Behrensmeyer, Eds. (Springer, 2007), pp. 129–157.
45. J. Rowan, E. D. Lorenzen, F. Bibi, "Evolutionary biogeography of African antelopes: Implications for *Paranthropus*" in *The Forgotten Lineage(s): Paleobiology of Paranthropus*, P. J. Constantino, K. E. Reed, B. A. Wood, Eds. (Springer), in press.
46. P. Bengtson, Open nomenclature. *Palaentology* **31**, 223–227 (1988).
47. T. M. Smiley, Detecting diversification rates in relation to preservation and tectonic history from simulated fossil records. *Paleobiology* **44**, 1–24 (2018).
48. J. D. Cryer, K. Chen, *Time Series Analysis with Applications in R* (Springer, ed. 2, 2008).
49. R. T. Dean, W. T. Dunsmuir, Dangers and uses of cross-correlation in analyzing time series in perception, performance, movement, and neuroscience: The importance of constructing transfer function autoregressive models. *Behav. Res. Methods* **48**, 783–802 (2016).
50. R Core Team, 2021 R: A language and environment for statistical computing. <https://www.r-project.org/>. Accessed 20 February 2022.
51. A. Du, J. Rowan, S. C. Wang, B. A. Wood, Z. Alemseged, Statistical estimates of hominin origination and extinction dates: A case study examining the *Australopithecus anamensis-afarensis* lineage. *J. Hum. Evol.* **138**, 102688 (2020).